Computer Aided Geometric Design 37 (2015) 42–56

Contents lists available at ScienceDirect

Computer Aided Geometric Design

www.elsevier.com/locate/cagd

A new B-spline representation for cubic splines over Powell–Sabin triangulations ☆

Hendrik Speleers

Department of Mathematics, University of Rome 'Tor Vergata', Via della Ricerca Scientifica, 00133 Rome, Italy

ARTICLE INFO

Article history:
Received 27 September 2014
Received in revised form 28 March 2015
Accepted 14 May 2015
Available online 27 May 2015

Keywords:
C^1 cubic splines
Macro-elements
Powell–Sabin splines
Clough–Tocher splines
Normalized B-splines
Bézier control net

ABSTRACT

We consider a C^1 cubic spline space defined over a triangulation with Powell–Sabin refinement. The space has some local C^2 super-smoothness and can be seen as a close extension of the classical cubic Clough–Tocher spline space. In addition, we construct a suitable normalized B-spline representation for this spline space. The basis functions have a local support, they are nonnegative, and they form a partition of unity. We also show how to compute the Bézier control net of such a spline in a stable way.

1. Introduction

Smooth (finite element) spline spaces defined over triangulations have been studied extensively and applied in different contexts (see, e.g., Lai and Schumaker, 2007; Nürnberger and Zeilfelder, 2000, and the references quoted therein). Typically, such spline spaces provide good approximation properties and possess a small dimension which can be expressed in terms of geometrically interesting characteristics of the triangulation (like the number of vertices, edges and/or triangles). In addition, a stable basis representation is often required for practical purposes.

For the construction of smooth splines with a low polynomial degree, one often considers triangulations with a particular macro-structure. Each triangle in the triangulation is then split into a number of subtriangles. The Clough–Tocher split (into three subtriangles) and the Powell–Sabin split (into six subtriangles) are commonly used splits. Splines defined on such refined triangulations are referred to as Clough–Tocher splines and Powell–Sabin splines, respectively.

Dierckx (1997) has developed an interesting normalized B-spline representation for C^1 quadratic Powell–Sabin splines. These splines have been introduced by Powell and Sabin (1977) with the aim of drawing contour lines of bivariate functions. The B-spline representation consists of a set of locally supported basis functions which form a convex partition of unity (i.e., they are nonnegative and sum up to one). The spline coefficients in this representation possess an intuitive geometric interpretation involving tangent control triangles. This normalized B-spline representation has been effective in a wide range of application areas, for example, surface modeling and compression (Dierckx, 1997; Maes and Bultheel, 2006; Speleers et al., 2009), scattered data interpolation and approximation (Manni and Sablonnière, 2007; Sbibih et al., 2009, 2015), the numerical solution of differential problems (Speleers et al., 2006, 2012). Recently, basis functions with similar properties have been constructed for certain Powell–Sabin spline spaces of higher degree and smoothness. In particular, we mention

☆ This paper has been recommended for acceptance by Oleg Davydov.
E-mail address: speleers@mat.uniroma2.it.

http://dx.doi.org/10.1016/j.cagd.2015.05.002

C^1 cubics (Lamnii et al., 2014), C^2 quintics (Speleers, 2010a), and a family of splines of smoothness r and polynomial degree $3r-1$ (Speleers, 2013a). Local super-smoothness has been imposed in order to simplify their construction and to reduce their number of degrees of freedom while maintaining the full approximation order. The quadratic Powell–Sabin spline case has also been extended to the trivariate setting (Sbibih et al., 2012) and the general multivariate setting (Speleers, 2013b).

On the other hand, the construction of a normalized B-spline representation for Clough–Tocher splines is a challenging task. Originally, C^1 cubic Clough–Tocher splines (CT3-splines) have been developed by Clough and Tocher (1965) as a tool for the finite element method. Later on, they were also applied in the area of scattered data interpolation (see, e.g., Farin, 1985; Kashyap, 1996; Mann, 1999). A normalized B-spline basis has been constructed by Speleers (2010b) for a certain subspace of the CT3-spline space. Yet, it is still an open question whether or not it is possible to construct a normalized B-spline basis for the full CT3-spline space. In this paper, we do not answer this question, but we provide a normalized B-spline basis for a slightly enlarged space, so every CT3-spline can be represented with it. We consider a C^1 cubic spline space defined over a triangulation endowed with a Powell–Sabin refinement. The space has specific local C^2 super-smoothness to mimic closely the CT3-spline space.

The paper is organized as follows. In Section 2 we review some general concepts of polynomials on triangles, we give the definition of our cubic spline space and point out its relation with the classical Clough–Tocher spline space. Section 3 covers the construction of a normalized B-spline basis and gives a geometric interpretation: we are looking for a set of triangles that contain a specific set of points. In Section 4 we consider spline surfaces and describe how control points can be defined. We also present a stable way to compute the Bézier ordinates of such a spline. Section 5 discusses some strategies to reduce the number of degrees of freedom in the proposed spline space. In particular, we detail the relation with the reduced CT3-splines developed by Speleers (2010b). Finally, in Section 6 we end with some concluding remarks.

2. C^1 cubic splines

In this section we introduce our C^1 cubic spline space. To this end, we first recall some preliminary concepts of bivariate polynomials in Bernstein–Bézier form defined on triangles.

2.1. Bivariate polynomials in Bernstein–Bézier representation

Let $\mathcal{T}(V_1, V_2, V_3)$ be a non-degenerate triangle. Any point P in the plane of the triangle can be uniquely expressed in terms of the barycentric coordinates $\tau = (\tau_1, \tau_2, \tau_3)$ with respect to $\mathcal{T}$, such that

$$P = \sum_{i=1}^{3} \tau_i V_i, \qquad \text{and} \qquad \tau_1 + \tau_2 + \tau_3 = 1. \tag{2.1}$$

Let $\mathbb{P}_d$ denote the linear space of bivariate polynomials of total degree less than or equal to d. Any polynomial $p_d \in \mathbb{P}_d$ defined over the triangle $\mathcal{T}$ has a unique Bernstein–Bézier representation

$$p_d(\tau) = \sum_{i+j+k=d} b_{ijk} B^d_{ijk}(\tau), \tag{2.2}$$

with

$$B^d_{ijk}(\tau) = \frac{d!}{i!j!k!} {\tau_1}^i {\tau_2}^j {\tau_3}^k \tag{2.3}$$

the Bernstein polynomials of degree d, which form a convex partition of unity on $\mathcal{T}$. The coefficients b_{ijk} are called Bézier ordinates, and the Bézier domain points ξ_{ijk} are defined as the points with barycentric coordinates $\left(\frac{i}{d}, \frac{j}{d}, \frac{k}{d}\right)$. The Bernstein–Bézier representation is often visualized in a schematic way by associating each Bézier ordinate b_{ijk} with the Bézier domain point ξ_{ijk}. The piecewise linear interpolant of the Bézier control points, defined as $\mathbf{b}_{ijk} = (\xi_{ijk}, b_{ijk})$, is called the Bézier control net. This control net is tangent to the polynomial surface at the three vertices. Polynomials in their Bernstein–Bézier form can be evaluated in a stable way using the de Casteljau algorithm. This algorithm can also be used to derive smoothness conditions between (the Bézier ordinates of) polynomials defined over adjacent triangles. More details can be found in the works by Farin (1986), Lai and Schumaker (2007).

The disk D_r of radius r around vertex V_1 of $\mathcal{T}$ is the set of domain points defined by

$$D_r(V_1) = \{\xi_{i_1 i_2 i_3} : i_1 \geq d - r\}. \tag{2.4}$$

The row E_r at distance r parallel to edge $\varepsilon_{12} = \langle V_1, V_2 \rangle$ in $\mathcal{T}$ is the set of domain points defined by

$$E_r(\varepsilon_{12}) = \{\xi_{i_1 i_2 i_3} : i_3 = r\}.$$

Given a triangulation Δ, the disk $D_r(V_1)$ in Δ is defined as the set of all domain points in (2.4) for each triangle in Δ having V_1 as a vertex. A row in Δ is defined in a similar way. Hereinafter, if we refer to a Bézier ordinate in a disk or on a row, then we actually mean a Bézier ordinate whose corresponding domain point is in that location.

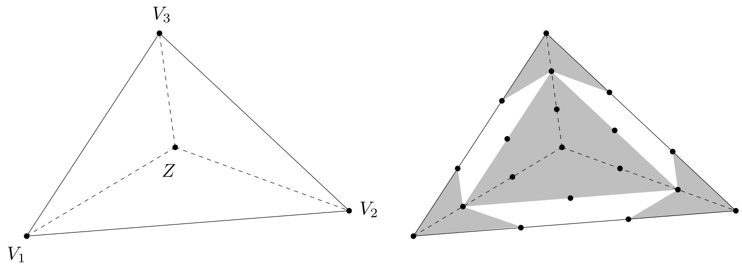

Fig. 1. Left: A Clough–Tocher split of a triangle $\mathcal{T}(V_1, V_2, V_3)$. Right: Bézier domain points and schematic representation of the inherent smoothness conditions (shaded regions) for $\mathbb{S}_3^1(\Delta_{CT})$.

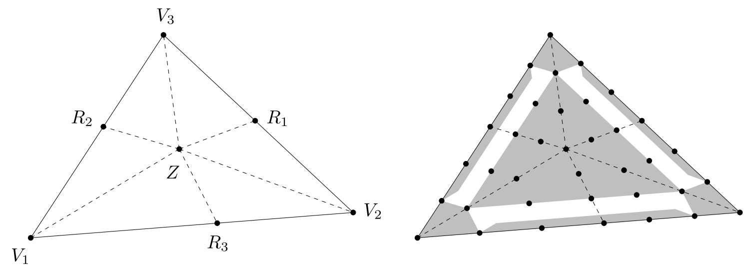

Fig. 2. Left: A Powell–Sabin split of a triangle $\mathcal{T}(V_1, V_2, V_3)$. Right: Bézier domain points and schematic representation of the inherent smoothness conditions (shaded regions) for $\widehat{\mathbb{S}}_3^1(\Delta_{PS})$.

2.2. The PS3-spline space

Let Ω be a closed polygonal domain in $\mathbb{R}^2$ and let Δ be a triangulation of Ω. We denote by n_v, n_t and n_e the number of vertices, triangles and edges in Δ, respectively. The vertices V_i, $i = 1, \dots, n_v$, in Δ have as Cartesian coordinates (x_i, y_i).

A Clough–Tocher (CT-) refinement Δ_{CT} of Δ partitions all triangles in Δ into three smaller triangles (Clough and Tocher, 1965). For each triangle $\mathcal{T}$, a split point Z is chosen in the interior of $\mathcal{T}$ and it is connected to the three vertices of $\mathcal{T}$ by straight lines (see Fig. 1(left)). The space of piecewise cubic polynomials on Δ_{CT} with global C^1-continuity will be referred to as the cubic Clough–Tocher (CT3-) spline space, i.e.,

$$\mathbb{S}_3^1(\Delta_{CT}) = \left\{ s \in C^1(\Omega) : s|_{\mathcal{T}_{CT}} \in \mathbb{P}_3,\ \mathcal{T}_{CT} \in \Delta_{CT} \right\}. \tag{2.5}$$

The dimension of this space is equal to $3n_v + n_e$. Given a single macro-triangle $\mathcal{T}(V_1, V_2, V_3)$ in Δ, on each of the three subtriangles the CT3-spline is a cubic polynomial that can be represented in its Bernstein–Bézier form, i.e., with $d = 3$ in equations (2.2) and (2.3). Fig. 1(right) shows the regions inside a macro-triangle where the corresponding Bézier ordinates of a CT3-spline are related by the inherent smoothness conditions. Note that CT3-splines possess a C^2 super-smoothness at the split points (see, e.g., Farin, 1986).

A Powell–Sabin (PS-) refinement Δ_{PS} of Δ is the refined triangulation obtained by subdividing each triangle of Δ into six subtriangles as follows (Powell and Sabin, 1977).

1. Select a split point Z_j inside each triangle $\mathcal{T}_j \in \Delta$ and connect it to the three vertices of $\mathcal{T}_j$ by straight lines.
2. For each pair of triangles $\mathcal{T}_i$ and $\mathcal{T}_j$ with a common edge, connect the two points Z_i and Z_j. If T_j is a boundary triangle, then also connect Z_j to an arbitrary point on each of the boundary edges.

These triangle split points must be chosen so that each constructed line segment $\langle Z_i, Z_j \rangle$ intersects the common edge of $\mathcal{T}_i$ and $\mathcal{T}_j$. Such a choice is always possible: for instance, one can take Z_j as the incenter (i.e., the center of the inscribed circle) of $\mathcal{T}_j$. The obtained split points on the edges ε_k, $k = 1, \dots, n_e$ are denoted by R_k as illustrated in Fig. 2(left).

The space of piecewise cubic polynomials on Δ_{PS} with global C^1-continuity is denoted by

$$\mathbb{S}_3^1(\Delta_{PS}) = \left\{ s \in C^1(\Omega) : s|_{\mathcal{T}_{PS}} \in \mathbb{P}_3,\ \mathcal{T}_{PS} \in \Delta_{PS} \right\}. \tag{2.6}$$

In this paper we focus on a particular subspace of $\mathbb{S}_3^1(\Delta_{PS})$ with additional smoothness around some vertices and edges. Imposing local super-smoothness is an interesting way to reduce the dimension of the space, while maintaining the full approximation order. Let $\mathcal{Z}_{PS} = \{Z_i\}_{i=1}^{n_t}$ be the set of triangle split points in Δ_{PS}, and let $\mathcal{E}_{PS}$ be the set of all edges in Δ_{PS} that connect a triangle split point Z_i to an edge split point R_k. The space $\widehat{\mathbb{S}}_3^1(\Delta_{PS})$ of super-smooth splines on Δ_{PS} is defined by

$$\widehat{\mathbb{S}}_3^1(\Delta_{PS}) = \left\{ s \in \mathbb{S}_3^1(\Delta_{PS}) : \; s \in C^2(Z), \; Z \in \mathcal{Z}_{PS}; \; s \in C^2(\varepsilon), \; \varepsilon \in \mathcal{E}_{PS} \right\}. \tag{2.7}$$

Here, $C^\mu(Z)$ means that the polynomials on triangles in Δ_{PS} sharing the vertex Z have common derivatives up to order μ at that vertex. Analogously, $C^\mu(\varepsilon)$ means that the polynomials on triangles in Δ_{PS} sharing the edge ε have common derivatives up to order μ along that edge. The space $\widehat{\mathbb{S}}_3^1(\Delta_{PS})$ will be referred to as the cubic Powell–Sabin (PS3-) spline space. Fig. 2(right) shows the regions inside a macro-triangle where the corresponding Bézier ordinates of a PS3-spline are related by the inherent smoothness conditions. A spline $s \in \widehat{\mathbb{S}}_3^1(\Delta_{PS})$ can be characterized by means of the following Hermite interpolation problem.

Theorem 1. *For each edge ε_m in Δ, let ν_m be any unit vector that is not parallel to the edge. There exists a unique spline $s(x, y) \in \widehat{\mathbb{S}}_3^1(\Delta_{PS})$ satisfying*

$$s(V_l) = f_l, \qquad \frac{\partial s}{\partial x}(V_l) = f_{x,l}, \qquad \frac{\partial s}{\partial y}(V_l) = f_{y,l}, \qquad l = 1, \dots, n_v, \tag{2.8a}$$

and

$$s(R_m) = g_m, \qquad \frac{\partial s}{\partial \nu_m}(R_m) = g_{\nu,m}, \qquad m = 1, \dots, n_e, \tag{2.8b}$$

for a given set of $(f_l, f_{x,l}, f_{y,l})$-values and $(g_m, g_{\nu,m})$-values. Hence, a PS3-spline is uniquely defined by means of its function value and first derivatives at the n_v vertices V_l in Δ and by means of its function value and ν_m-derivative at the n_e edge split points R_m in Δ_{PS}.

Proof. We focus on a single macro-triangle $\mathcal{T}(V_1, V_2, V_3)$ in Δ, as shown in Fig. 2. On each of the six subtriangles, the PS3-spline s is a cubic polynomial that can be represented in its Bernstein–Bézier form. We will check that the interpolation conditions in (2.8) uniquely specify all the Bézier ordinates of s on the macro-triangle. The conditions (2.8a) determine the Bézier ordinates in the disks $D_1(V_1)$, $D_1(V_2)$ and $D_1(V_3)$. Because of the C^2-smoothness across the edge $\langle Z, R_3 \rangle$ and the conditions (2.8b) at the split point R_3 on the edge $\varepsilon_3 = \langle V_1, V_2 \rangle$, the remaining Bézier ordinates on the rows $E_r(\varepsilon_3)$, $r = 0, 1$ are also uniquely defined. The same argument holds for the Bézier ordinates on the rows related to the edges $\varepsilon_1 = \langle V_2, V_3 \rangle$ and $\varepsilon_2 = \langle V_3, V_1 \rangle$. Finally, the C^2 smoothness at the split point Z specifies the remaining Bézier ordinates in the disk $D_2(Z)$. $\square$

From Theorem 1 it follows that the dimension of $\widehat{\mathbb{S}}_3^1(\Delta_{PS})$ is equal to $3n_v + 2n_e$.

In the next theorem we show that the CT3-spline space is a subspace of the PS3-spline space. We say that the partitions Δ_{CT} and Δ_{PS} of the same triangulation Δ are compatible if the triangle split points Z_i, $i = 1, \dots, n_t$ coincide in both partitions.

Theorem 2. *If the partitions Δ_{CT} and Δ_{PS} are compatible, then*

$$\mathbb{S}_3^1(\Delta_{CT}) \subset \widehat{\mathbb{S}}_3^1(\Delta_{PS}).$$

Proof. It is easy to see that $\widetilde{\mathbb{S}}_3^1(\Delta_{PS}) \subset \widehat{\mathbb{S}}_3^1(\Delta_{PS})$, where

$$\widetilde{\mathbb{S}}_3^1(\Delta_{PS}) = \left\{ s \in \mathbb{S}_3^1(\Delta_{PS}) : \; s \in C^2(Z), \; Z \in \mathcal{Z}_{PS}; \; s \in C^3(\varepsilon), \; \varepsilon \in \mathcal{E}_{PS} \right\}.$$

We now show that $\widetilde{\mathbb{S}}_3^1(\Delta_{PS}) = \mathbb{S}_3^1(\Delta_{CT})$ when the partitions Δ_{CT} and Δ_{PS} are compatible. As already mentioned before, the CT3-splines possess a C^2 super-smoothness at the split points $Z \in \mathcal{Z}_{PS}$. Moreover, when a cubic spline is C^3 across an interior edge $\varepsilon \in \mathcal{E}_{PS}$, it is a single cubic polynomial over the two adjacent subtriangles. This completes the proof. $\square$

Since the CT3-spline space is a subspace of the PS3-spline space, the latter space also contains cubic polynomials, and consequently has an optimal approximation order.

Another cubic subspace of $\mathbb{S}_3^1(\Delta_{PS})$ with local C^2 super-smoothness has been considered by Chen and Liu (2008); Lamnii et al. (2014). However, that space is not so attractive as (2.7), because the corresponding Hermite interpolation scheme involves second order derivatives and the CT3-spline space is not a subspace. Many other spline spaces with a higher order of smoothness defined on a triangulation with PS-refinement or CT-refinement can be found in the literature (see, e.g., Alfeld and Schumaker, 2002a, 2002b; Laghchim-Lahlou and Sablonnière, 1994; Lai and Schumaker, 2001, 2003, 2007; Sablonnière, 1985; Speleers, 2013a).

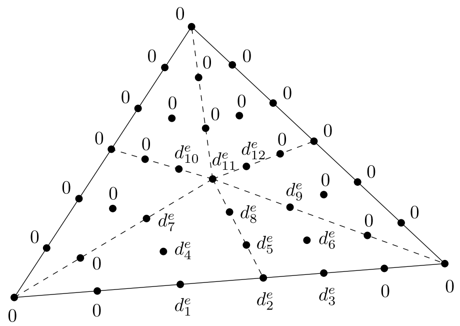

Fig. 3. Schematic representation of the Bézier ordinates of a B-spline with respect to an edge.

3. A normalized B-spline representation for PS3-splines

In this section we look for a suitable B-spline representation of $s(x, y) \in \widehat{\mathbb{S}}_3^1(\Delta_{PS})$,

$$s(x, y) = \sum_{i=1}^{n_v} \sum_{j=1}^{3} c^v_{i,j} B^v_{i,j}(x, y) + \sum_{k=1}^{n_e} \sum_{j=1}^{2} c^e_{k,j} B^e_{k,j}(x, y), \tag{3.1}$$

in which the basis functions $B^v_{i,j}(x, y)$ and $B^e_{k,j}(x, y)$ have a local support and form a convex partition of unity. We will refer to $B^v_{i,j}(x, y)$ and $B^e_{k,j}(x, y)$ as a B-spline with respect to the vertex V_i and the edge ε_k, respectively.

3.1. A B-spline with respect to an edge

We define the B-spline $B^e_{k,j}(x, y)$ with respect to the edge ε_k as the unique solution of the interpolation problem (2.8) with all $(f_l, f_{x,l}, f_{y,l}) = (0, 0, 0)$ and with all $(g_m, g_{\nu,m}) = (0, 0)$, except for $m = k$, where $(g_k, g_{\nu,k}) \neq (0, 0)$. It is easy to prove that such a spline vanishes outside the union of the two macro-triangles adjacent to the edge ε_k.

We now focus on the macro-triangle $\mathcal{T}(V_1, V_2, V_3)$, as shown in Fig. 2(left), and we assume that the points indicated in the figure have the following barycentric coordinates:

$$\begin{aligned}
&V_1 = (1, 0, 0), \qquad V_2 = (0, 1, 0), \qquad V_3 = (0, 0, 1), \qquad Z = (z_1, z_2, z_3),\\
&R_1 = (0, \lambda_{23}, \lambda_{32}), \qquad R_2 = (\lambda_{13}, 0, \lambda_{31}), \qquad R_3 = (\lambda_{12}, \lambda_{21}, 0).
\end{aligned} \tag{3.2}$$

In order to specify completely the B-spline $B^e_{k,j}(x, y)$ related to the edge $\varepsilon_3 = \langle V_1, V_2\rangle$ $(k = 3)$, i.e., determining the values $(g_k, g_{\nu,k})$, we make use of the Bernstein–Bézier representation. The corresponding Bézier ordinates are schematically represented in Fig. 3. From the definition of the B-spline it follows that many of these ordinates are zero, as can be seen in the figure. Because of the C^2-continuity across the edge $\langle Z, R_3\rangle$, the Bézier ordinates d^e_1, d^e_2, d^e_3 can be regarded as ordinates after subdivision of a single (univariate) quadratic polynomial p^e_2 defined on the edge segment $\langle P_1, P_2\rangle$ given by

$$P_1 = \frac{2}{3}V_1 + \frac{1}{3}R_3, \qquad P_2 = \frac{2}{3}V_2 + \frac{1}{3}R_3. \tag{3.3}$$

This quadratic polynomial p^e_2 can be chosen to have the values $0, \beta_{k,j}, 0$ as its three Bézier ordinates, for some parameter $\beta_{k,j}$. Then, we get

$$d^e_1 = \lambda_{21}\beta_{k,j}, \qquad d^e_2 = 2\lambda_{12}\lambda_{21}\beta_{k,j}, \qquad d^e_3 = \lambda_{12}\beta_{k,j}. \tag{3.4}$$

In a similar way, we obtain

$$d^e_4 = \lambda_{21}\gamma_{k,j}, \qquad d^e_5 = 2\lambda_{12}\lambda_{21}\gamma_{k,j}, \qquad d^e_6 = \lambda_{12}\gamma_{k,j}, \tag{3.5}$$

for some parameter $\gamma_{k,j}$. The remaining ordinates are determined by the C^2-smoothness at the split point Z, i.e.,

$$\begin{aligned}
&d^e_7 = z_2\gamma_{k,j}, \qquad d^e_8 = (z_2\lambda_{12} + z_1\lambda_{21})\gamma_{k,j}, \qquad d^e_9 = z_1\gamma_{k,j},\\
&d^e_{10} = z_2\lambda_{13}\gamma_{k,j}, \qquad d^e_{11} = 2z_1z_2\gamma_{k,j}, \qquad d^e_{12} = z_1\lambda_{23}\gamma_{k,j}.
\end{aligned} \tag{3.6}$$

In order to ensure nonnegativity, it suffices to impose that all Bézier ordinates of the B-spline $B^e_{k,j}(x, y)$ are nonnegative. Looking at (3.4)–(3.6), this is the case when

$$\beta_{k,j} \geq 0, \qquad \gamma_{k,j} \geq 0. \tag{3.7}$$

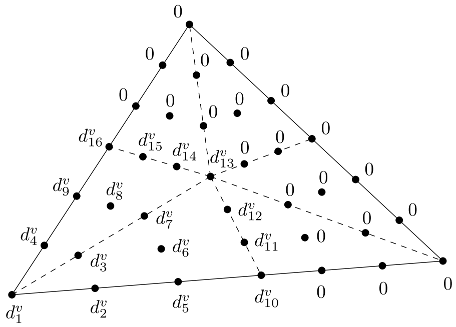

Fig. 4. Schematic representation of the Bézier ordinates of a B-spline with respect to a vertex.

The conditions in (3.7) are also necessary conditions for nonnegativity, because $B^e_{k,j}(R_k) = d^e_2 = 2\lambda_{12}\lambda_{21}\beta_{k,j}$ and $B^e_{k,j}(Z) = d^e_{11} = 2z_1z_2\gamma_{k,j}$. Hence, we need to choose two couples of parameters $(\beta_{k,1}, \gamma_{k,1})$ and $(\beta_{k,2}, \gamma_{k,2})$ satisfying (3.7) in order to define two nonnegative basis functions related to the edge ε_k. Depending on the type of the edge ε_k, we choose these parameters as follows.

1. If ε_k is a boundary edge:

$$(\beta_{k,1}, \gamma_{k,1}) = (0, 1), \qquad \text{and} \qquad (\beta_{k,2}, \gamma_{k,2}) = (1, 0). \tag{3.8a}$$

2. If ε_k is an interior edge, so that there is another adjacent macro-triangle $\widetilde{\mathcal{T}}$ and the line through the split points Z and $\widetilde{Z}$ intersects the edge in R_k:

$$(\beta_{k,1}, \gamma_{k,1}) = \left(\frac{\|R_k - \widetilde{Z}\|}{\|Z - \widetilde{Z}\|}, 1\right), \qquad \text{and} \qquad (\beta_{k,2}, \gamma_{k,2}) = \left(\frac{\|Z - R_k\|}{\|Z - \widetilde{Z}\|}, 0\right). \tag{3.8b}$$

Note that in both cases

$$\beta_{k,1} + \beta_{k,2} = 1, \qquad \gamma_{k,1} + \gamma_{k,2} = 1.$$

3.2. A B-spline with respect to a vertex

The molecule (also called 1-ring) M_i of the vertex V_i is defined as the union of all triangles in the triangulation that contain V_i. The B-spline $B^v_{i,j}(x, y)$ with respect to the vertex V_i is defined as the unique solution of the interpolation problem (2.8) with all $(f_l, f_{x,l}, f_{y,l}) = (0, 0, 0)$, except for $l = i$, where $(f_i, f_{x,i}, f_{y,i}) = (\alpha_{i,j}, \alpha^x_{i,j}, \alpha^y_{i,j})$, and with all $(g_m, g_{\nu,m}) = (0, 0)$, except for any m such that ε_m is an edge with V_i as endpoint, where $(g_m, g_{\nu,m}) \neq (0, 0)$. Such a spline is zero outside the molecule of V_i.

We consider again the macro-triangle $\mathcal{T}(V_1, V_2, V_3)$ depicted in Fig. 2(left); the barycentric coordinates of the points in the figure are given in (3.2). Without loss of generality, we look at the Bernstein–Bézier representation of the B-spline $B^v_{1,j}(x, y)$ related to the vertex V_1 $(i = 1)$, in order to specify the values $(g_m, g_{\nu,m})$ assuming the triplet $(\alpha_{1,j}, \alpha^x_{1,j}, \alpha^y_{1,j})$ is given. The corresponding Bézier ordinates are schematically represented in Fig. 4. In view of the C^1-smoothness at the vertex V_1, the Bézier ordinates in the neighborhood of V_1 are found as

$$d^v_1 = \alpha_{1,j}, \tag{3.9a}$$

$$d^v_2 = \alpha_{1,j} + \frac{\lambda_{21}}{3}\left(\alpha^x_{1,j}(x_2 - x_1) + \alpha^y_{1,j}(y_2 - y_1)\right), \tag{3.9b}$$

$$d^v_3 = \alpha_{1,j} + \frac{z_2}{3}\left(\alpha^x_{1,j}(x_2 - x_1) + \alpha^y_{1,j}(y_2 - y_1)\right) + \frac{z_3}{3}\left(\alpha^x_{1,j}(x_3 - x_1) + \alpha^y_{1,j}(y_3 - y_1)\right), \tag{3.9c}$$

$$d^v_4 = \alpha_{1,j} + \frac{\lambda_{31}}{3}\left(\alpha^x_{1,j}(x_3 - x_1) + \alpha^y_{1,j}(y_3 - y_1)\right). \tag{3.9d}$$

In a similar way we can compute the Bézier ordinates in the neighborhood of the vertices V_2 and V_3. In order to satisfy the C^2-continuity across the edge $\langle Z, R_3\rangle$, we take

$$d^v_5 = \lambda_{12} d^v_2, \qquad d^v_6 = \lambda_{12} d^v_3, \qquad d^v_{10} = \lambda_{12}{}^2 d^v_2, \qquad d^v_{11} = \lambda_{12}{}^2 d^v_3. \tag{3.10}$$

Note that the ordinates d^v_2, d^v_5, d^v_{10} can be regarded as ordinates after subdivision of a single (univariate) quadratic polynomial p^v_2 defined on the edge segment $\langle P_1, P_2\rangle$, see (3.3). This quadratic polynomial p^v_2 has the values $d^v_2, 0, 0$ as its three Bézier ordinates. A similar reasoning holds for the ordinates d_3^v, d_6^v, d_{11}^v. In the same way, in order to satisfy the C^2-continuity across the edge $\langle Z, R_2\rangle$, we take

$$d_9^v = \lambda_{13} d_4^v, \qquad d_8^v = \lambda_{13} d_3^v, \qquad d_{16}^v = \lambda_{13}{}^2 d_4^v, \qquad d_{15}^v = \lambda_{13}{}^2 d_3^v. \tag{3.11}$$

The remaining Bézier ordinates are then specified by the C^2-smoothness at the split point Z, i.e.,

$$d_7^v = z_1 d_3^v, \qquad d_{12}^v = z_1 \lambda_{12} d_3^v, \qquad d_{13}^v = z_1{}^2 d_3^v, \qquad d_{14}^v = z_1 \lambda_{13} d_3^v. \tag{3.12}$$

From the Bernstein–Bézier representation depicted in Fig. 4 we notice that the B-spline $B_{1,j}^v(x,y)$ is C^2-continuous across the edge $\langle V_2, V_3\rangle$.

In order to ensure nonnegativity of $B_{1,j}^v(x,y)$, we impose that all its Bézier ordinates are nonnegative. It is clear from (3.9)–(3.12), that this is the case when

$$d_1^v \geq 0, \qquad d_2^v \geq 0, \qquad d_3^v \geq 0, \qquad d_4^v \geq 0. \tag{3.13}$$

This is not only a sufficient condition, but also a necessary condition for nonnegativity. Indeed, we have $B_{1,j}^v(V_i) = d_1^v$, $B_{1,j}^v(R_3) = d_{10}^v = \lambda_{12}{}^2 d_2^v$, $B_{1,j}^v(R_2) = d_{16}^v = \lambda_{13}{}^2 d_4^v$, and $B_{1,j}^v(Z) = d_{13}^v = z_1{}^2 d_3^v$. If the molecule of V_1 has more than one triangle, then we have to impose conditions similar to (3.13) for each of these triangles. These conditions are always feasible and there is an infinite number of solutions. This can be proved following the same geometric construction as developed by Dierckx (1997); the details are given in the next subsection.

3.3. A geometric approach to form a convex partition of unity

In this subsection we investigate for which choices of the parameters $(\alpha_{i,j}, \alpha_{i,j}^x, \alpha_{i,j}^y)$ the basis functions form a convex partition of unity. From the definition of the B-splines (related to both the vertices and the edges) it follows that only three basis functions have a nonzero function and derivative value at the vertex V_i. Hence, we need to satisfy

$$\alpha_{i,1} + \alpha_{i,2} + \alpha_{i,3} = 1, \tag{3.14a}$$
$$\alpha_{i,1}^x + \alpha_{i,2}^x + \alpha_{i,3}^x = 0, \tag{3.14b}$$
$$\alpha_{i,1}^y + \alpha_{i,2}^y + \alpha_{i,3}^y = 0, \tag{3.14c}$$

for $i = 1, \ldots, n_v$. By taking into account the construction of the B-splines and the choices for the edge parameters in (3.8), we easily find that the conditions (3.14) are necessary and sufficient to form a partition of unity.

We now focus on the nonnegativity of the basis functions. For each vertex V_i we define three points $Q_{i,j}^v = (X_{i,j}^v, Y_{i,j}^v)$, $j = 1, 2, 3$, and for each edge ε_k we define two points $Q_{k,j}^e = (X_{k,j}^e, Y_{k,j}^e)$, $j = 1, 2$, such that

$$\sum_{i=1}^{n_v} \sum_{j=1}^{3} X_{i,j}^v B_{i,j}^v(x,y) + \sum_{k=1}^{n_e} \sum_{j=1}^{2} X_{k,j}^e B_{k,j}^e(x,y) = x, \tag{3.15a}$$
$$\sum_{i=1}^{n_v} \sum_{j=1}^{3} Y_{i,j}^v B_{i,j}^v(x,y) + \sum_{k=1}^{n_e} \sum_{j=1}^{2} Y_{k,j}^e B_{k,j}^e(x,y) = y, \tag{3.15b}$$

for any $(x, y) \in \Omega$. Hence, the points $Q_{i,j}^v$ and $Q_{k,j}^e$ are the Greville points for our B-spline representation. By using the interpolation problem (2.8) and the definition of the B-splines, the Cartesian coordinates of the points $Q_{i,j}^v$ can be obtained as the solution of the systems

$$\alpha_{i,1} X_{i,1}^v + \alpha_{i,2} X_{i,2}^v + \alpha_{i,3} X_{i,3}^v = x_i, \tag{3.16a}$$
$$\alpha_{i,1}^x X_{i,1}^v + \alpha_{i,2}^x X_{i,2}^v + \alpha_{i,3}^x X_{i,3}^v = 1, \tag{3.16b}$$
$$\alpha_{i,1}^y X_{i,1}^v + \alpha_{i,2}^y X_{i,2}^v + \alpha_{i,3}^y X_{i,3}^v = 0, \tag{3.16c}$$

and

$$\alpha_{i,1} Y_{i,1}^v + \alpha_{i,2} Y_{i,2}^v + \alpha_{i,3} Y_{i,3}^v = y_i, \tag{3.17a}$$
$$\alpha_{i,1}^x Y_{i,1}^v + \alpha_{i,2}^x Y_{i,2}^v + \alpha_{i,3}^x Y_{i,3}^v = 0, \tag{3.17b}$$
$$\alpha_{i,1}^y Y_{i,1}^v + \alpha_{i,2}^y Y_{i,2}^v + \alpha_{i,3}^y Y_{i,3}^v = 1. \tag{3.17c}$$

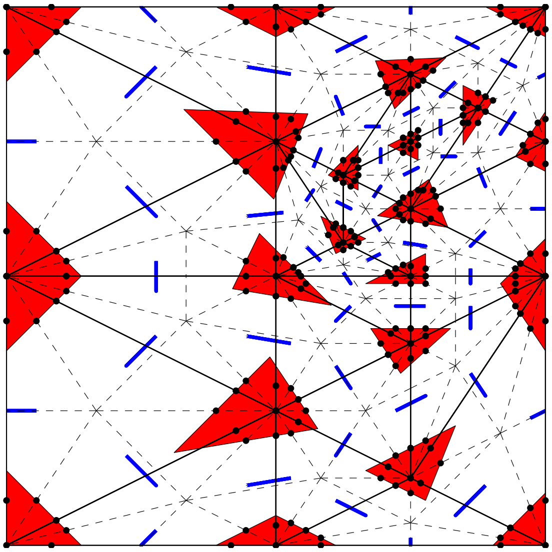

Fig. 5. A PS-refined triangulation with a set of optimal PS3-triangles (red) and PS3-lines (blue). (For interpretation of the references to color in this figure legend, the reader is referred to the web version of this article.)

We can compactly write (3.14), (3.16) and (3.17) in the following matrix notation

$$\begin{bmatrix} \alpha_{i,1} & \alpha_{i,2} & \alpha_{i,3} \\ \alpha^x_{i,1} & \alpha^x_{i,2} & \alpha^x_{i,3} \\ \alpha^y_{i,1} & \alpha^y_{i,2} & \alpha^y_{i,3} \end{bmatrix} \begin{bmatrix} X^v_{i,1} & Y^v_{i,1} & 1 \\ X^v_{i,2} & Y^v_{i,2} & 1 \\ X^v_{i,3} & Y^v_{i,3} & 1 \end{bmatrix} = \begin{bmatrix} x_i & y_i & 1 \\ 1 & 0 & 0 \\ 0 & 1 & 0 \end{bmatrix}. \tag{3.18}$$

The triangle $t_i(Q^v_{i,1}, Q^v_{i,2}, Q^v_{i,3})$ will be called the PS3-triangle with respect to the vertex V_i.

Following the same arguments as for quadratic Powell–Sabin B-splines (Dierckx, 1997), it can be easily shown that the constraints (3.13) related to the macro-triangle $\mathcal{T}(V_1, V_2, V_3)$ are equivalent to the request that the following set of points are inside the triangle t_1:

$$V_1, \qquad S_1 = \frac{2}{3}V_1 + \frac{1}{3}Z, \qquad S_2 = \frac{2}{3}V_1 + \frac{1}{3}R_2, \qquad S_3 = \frac{2}{3}V_1 + \frac{1}{3}R_3. \tag{3.19}$$

These points are the Bézier domain points in the disk $D_1(V_1)$ in Δ_{PS}, and they will be called PS3-points with respect to the vertex V_1. Summarizing, we can state the following theorem.

Theorem 3. *The set of B-splines $B^v_{i,j}(x, y)$ and $B^e_{k,j}(x, y)$ are nonnegative and form a partition of unity, if the parameters $(\alpha_{i,j}, \alpha^x_{i,j}, \alpha^y_{i,j})$ and $(\beta_{k,j}, \gamma_{k,j})$ in their definitions are constructed as follows.*

1. *For each vertex V_i in Δ, the parameters $(\alpha_{i,j}, \alpha^x_{i,j}, \alpha^y_{i,j})$, $j = 1, 2, 3$, are determined by the relation (3.18), given a PS3-triangle $t_i(Q^v_{i,1}, Q^v_{i,2}, Q^v_{i,3})$ that contains all the corresponding PS3-points, i.e., the Bézier domain points in the disk $D_1(V_i)$ in Δ_{PS}.*
2. *For each edge ε_k in Δ, the parameters $(\beta_{k,j}, \gamma_{k,j})$, $j = 1, 2$, are given by (3.8).*

There are many triangles that contain all PS3-points. An appropriate choice for such triangles, as suggested by Dierckx (1997) and Speleers (2010b), is to calculate triangles of minimal area, the so-called optimal triangles. In Fig. 5 we illustrate the PS3-points (black bullets) and a set of optimal PS3-triangles (red triangles) for a triangulation taken from Dierckx et al. (1992). Note that such PS3-triangles are much smaller than the ones needed for quadratic Powell–Sabin B-splines and for reduced Clough–Tocher B-splines; we refer to Speleers (2010b, Fig. 5 and Fig. 6) for a comparison on the same triangulation.

Given the position of the points $Q^v_{i,j}$, the triplets $(\alpha_{i,j}, \alpha^x_{i,j}, \alpha^y_{i,j})$ can be computed as follows. Referring to (2.1) and (3.18), the values $(\alpha_{i,1}, \alpha_{i,2}, \alpha_{i,3})$ can be interpreted as the barycentric coordinates of the vertex V_i with respect to $t_i(Q^v_{i,1}, Q^v_{i,2}, Q^v_{i,3})$. From (3.18) we obtain that

$$\alpha^x_{i,1} = \frac{Y_{i,2} - Y_{i,3}}{F}, \qquad \alpha^x_{i,2} = \frac{Y_{i,3} - Y_{i,1}}{F}, \qquad \alpha^x_{i,3} = \frac{Y_{i,1} - Y_{i,2}}{F},$$
$$\alpha^y_{i,1} = \frac{X_{i,3} - X_{i,2}}{F}, \qquad \alpha^y_{i,2} = \frac{X_{i,1} - X_{i,3}}{F}, \qquad \alpha^y_{i,3} = \frac{X_{i,2} - X_{i,1}}{F},$$

with

$$F = \begin{vmatrix} X_{i,1} & Y_{i,1} & 1 \\ X_{i,2} & Y_{i,2} & 1 \\ X_{i,3} & Y_{i,3} & 1 \end{vmatrix}.$$

The triplets $(\alpha^x_{i,1}, \alpha^x_{i,2}, \alpha^x_{i,3})$ and $(\alpha^y_{i,1}, \alpha^y_{i,2}, \alpha^y_{i,3})$ can be seen as the barycentric coordinates of the x- and y-direction with respect to t_i.

Finally, we provide an expression for the points $Q^e_{k,j}$, $j = 1, 2$, related to the edges ε_k, $k = 1, \ldots, n_e$. By exploiting the Bernstein–Bézier representation of the B-splines and the parameter choices in (3.8), we deduce that

$$Q^e_{k,1} = \frac{1}{2}\left(\frac{2}{3}V_1 + \frac{1}{3}Z\right) + \frac{1}{2}\left(\frac{2}{3}V_2 + \frac{1}{3}Z\right) = \frac{1}{3}(V_1 + V_2 + Z),$$

for an edge $\varepsilon_k = \langle V_1, V_2\rangle$ belonging to the macro-triangle $\mathcal{T}$ which has the split point Z. A similar reasoning can be used for $Q^e_{k,2}$, and we arrive at the following expressions.

1. If $\varepsilon_k = \langle V_1, V_2\rangle$ is a boundary edge, having the split point R_k and belonging to the macro-triangle $\mathcal{T}$ which has the split point Z:

$$Q^e_{k,1} = \frac{1}{3}(V_1 + V_2 + Z), \qquad \text{and} \qquad Q^e_{k,2} = \frac{1}{3}(V_1 + V_2 + R_k). \tag{3.20a}$$

2. If $\varepsilon_k = \langle V_1, V_2\rangle$ is an interior edge, shared between the two macro-triangles $\mathcal{T}$ and $\widetilde{\mathcal{T}}$ having the split points Z and $\widetilde{Z}$, respectively:

$$Q^e_{k,1} = \frac{1}{3}(V_1 + V_2 + Z), \qquad \text{and} \qquad Q^e_{k,2} = \frac{1}{3}(V_1 + V_2 + \widetilde{Z}). \tag{3.20b}$$

The line segment $\ell_k(Q^e_{k,1}, Q^e_{k,2})$ will be called the PS3-line with respect to the edge ε_k. Fig. 5 depicts the PS3-lines (blue lines) for the given PS-refined triangulation.

4. PS3-spline surfaces

In this section we describe how to define control points and we provide a stable computation of the Bézier ordinates of a spline in the form (3.1). We assume that we are dealing with B-splines that are constructed as in Theorem 3.

4.1. Control points

Referring to the PS3-spline representation (3.1) and the definition of the points $Q^v_{i,j}$ and $Q^e_{k,j}$ in (3.15), we may define control points as

$$\mathbf{c}^v_{i,j} = (X^v_{i,j}, Y^v_{i,j}, c^v_{i,j}), \qquad j = 1, 2, 3, \qquad \text{and} \qquad \mathbf{c}^e_{k,j} = (X^e_{k,j}, Y^e_{k,j}, c^e_{k,j}), \qquad j = 1, 2, \tag{4.1}$$

for $i = 1, \ldots, n_v$ and $k = 1, \ldots, n_e$. We recall that the points $Q^v_{i,j}$ form the vertices of the PS3-triangles, whereas the expressions of the points $Q^e_{k,j}$ are given in (3.20). Since the PS3-spline basis forms a convex partition of unity, it follows that the graph of a spline in the form (3.1) lies inside the convex hull of the control points (4.1). The first set of control points can be considered as vertices of the triangles $T_i(\mathbf{c}^v_{i,1}, \mathbf{c}^v_{i,2}, \mathbf{c}^v_{i,3})$, $i = 1, \ldots, n_v$, which are called control triangles; the second set as vertices of the line segments $L_k(\mathbf{c}^e_{k,1}, \mathbf{c}^e_{k,2})$, $k = 1, \ldots, n_e$, which are called control lines.

From the definition of the B-splines we know that

$$s(V_i) = \alpha_{i,1}\, c^v_{i,1} + \alpha_{i,2}\, c^v_{i,2} + \alpha_{i,3}\, c^v_{i,3}, \tag{4.2a}$$

$$\frac{\partial s}{\partial x}(V_i) = \alpha^x_{i,1}\, c^v_{i,1} + \alpha^x_{i,2}\, c^v_{i,2} + \alpha^x_{i,3}\, c^v_{i,3}, \tag{4.2b}$$

$$\frac{\partial s}{\partial y}(V_i) = \alpha^y_{i,1}\, c^v_{i,1} + \alpha^y_{i,2}\, c^v_{i,2} + \alpha^y_{i,3}\, c^v_{i,3}. \tag{4.2c}$$

Inverting the system (4.2), and using (3.18), we find after some elementary calculations that

$$c^v_{i,1} = s(V_i) + (X^v_{i,1} - x_i)\frac{\partial s}{\partial x}(V_i) + (Y^v_{i,1} - y_i)\frac{\partial s}{\partial y}(V_i),$$

$$c^v_{i,2} = s(V_i) + (X^v_{i,2} - x_i)\frac{\partial s}{\partial x}(V_i) + (Y^v_{i,2} - y_i)\frac{\partial s}{\partial y}(V_i),$$

$$c^v_{i,3} = s(V_i) + (X^v_{i,3} - x_i)\frac{\partial s}{\partial x}(V_i) + (Y^v_{i,3} - y_i)\frac{\partial s}{\partial y}(V_i).$$

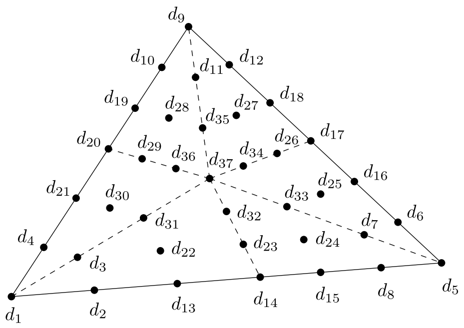

Fig. 6. Schematic representation of the Bézier ordinates of a PS3-spline.

It follows that the three control points $\mathbf{c}^v_{i,j}$, $j = 1, 2, 3$, belong to the plane tangent to the spline surface $z = s(x, y)$ at vertex V_i. Thus, the control triangle T_i is tangent to the spline surface at V_i. There is no similar tangent property for the control lines.

4.2. Bézier ordinates of a PS3-spline

The Bézier ordinates of a PS3-spline in the form (3.1) can be computed in a stable way from its B-spline coefficients $c^v_{i,j}$ and $c^e_{k,j}$. We illustrate this procedure on the macro-triangle $\mathcal{T}(V_1, V_2, V_3)$ shown in Fig. 2(left), and the corresponding Bézier ordinates are depicted in Fig. 6. The barycentric coordinates of the points in the macro-triangle are given in (3.2).

By combining the formulas (3.9) and (4.2), we derive that the Bézier ordinates in the disk $D_1(V_1)$ only depend on the three coefficients $c^v_{1,j}$ with $j = 1, 2, 3$:

$$\begin{aligned} d_1 &= \alpha_{1,1}\, c^v_{1,1} + \alpha_{1,2}\, c^v_{1,2} + \alpha_{1,3}\, c^v_{1,3}, \qquad & d_2 &= \sigma_{3,1}\, c^v_{1,1} + \sigma_{3,2}\, c^v_{1,2} + \sigma_{3,3}\, c^v_{1,3}, \\ d_3 &= \sigma_{1,1}\, c^v_{1,1} + \sigma_{1,2}\, c^v_{1,2} + \sigma_{1,3}\, c^v_{1,3}, \qquad & d_4 &= \sigma_{2,1}\, c^v_{1,1} + \sigma_{2,2}\, c^v_{1,2} + \sigma_{2,3}\, c^v_{1,3}, \end{aligned} \tag{4.3}$$

where $(\alpha_{1,1}, \alpha_{1,2}, \alpha_{1,3})$, $(\sigma_{1,1}, \sigma_{1,2}, \sigma_{1,3})$, $(\sigma_{2,1}, \sigma_{2,2}, \sigma_{2,3})$ and $(\sigma_{3,1}, \sigma_{3,2}, \sigma_{3,3})$ are the barycentric coordinates of the PS3-points V_1, S_1, S_2 and S_3, respectively, with respect to the PS3-triangle $t_1(Q^v_{1,1}, Q^v_{1,2}, Q^v_{1,3})$, see (3.19). The expressions in (4.3) are convex combinations since the PS3-points are required to be inside the PS3-triangle. In a similar way we can compute (d_5, d_6, d_7, d_8) and $(d_9, d_{10}, d_{11}, d_{12})$ from the B-spline coefficients $c^v_{2,j}$ and $c^v_{3,j}$, respectively.

The values of the Bézier ordinates d_{13}, d_{14}, d_{15} are computed from the C^2-smoothness conditions of the PS3-spline across the edge $\langle Z, R_3\rangle$. As we have already mentioned before, they can be regarded as ordinates after subdivision of a single (univariate) quadratic polynomial p_2 defined on the edge segment $\langle P_1, P_2\rangle$, see (3.3). This quadratic polynomial p_2 has the values d_2, β, d_8 as its three Bézier ordinates, where the value of β depends on the type of the edge ε_3.

1. If ε_k $(k = 3)$ is a boundary edge, then
$$\beta = c^e_{k,2}, \tag{4.4a}$$
following the B-spline ordering as in (3.8a).
2. If ε_k $(k = 3)$ is an interior edge, then
$$\beta = \frac{\|R_k - \widetilde{Z}\|}{\|Z - \widetilde{Z}\|}\, c^e_{k,1} + \frac{\|Z - R_k\|}{\|Z - \widetilde{Z}\|}\, c^e_{k,2}, \tag{4.4b}$$
following the same notation as in (3.8b).

Then, we find that

$$d_{13} = \lambda_{12} d_2 + \lambda_{21}\beta, \qquad d_{15} = \lambda_{12}\beta + \lambda_{21} d_8, \qquad d_{14} = \lambda_{12} d_{13} + \lambda_{21} d_{15}. \tag{4.5}$$

Similar expressions can be obtained for the Bézier ordinates $d_{16}, \ldots, d_{21}$.

Finally, the Bézier ordinates $d_{22}, \ldots, d_{37}$ can be computed by exploiting the C^2-smoothness at the split point Z. They can be regarded as ordinates after subdivision of a single (bivariate) quadratic polynomial $\hat{p}_2$ defined on the triangle spanned by the points

$$\widehat{P}_1 = \frac{2}{3}V_1 + \frac{1}{3}Z, \qquad \widehat{P}_2 = \frac{2}{3}V_2 + \frac{1}{3}Z, \qquad \widehat{P}_3 = \frac{2}{3}V_3 + \frac{1}{3}Z.$$

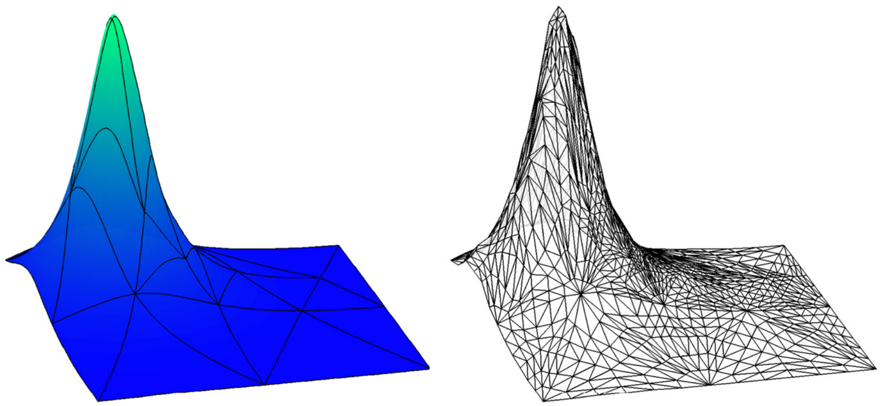

Fig. 7. Left: A PS3-spline surface together with the triangular mesh lines related to the triangulation in Fig. 5. Right: The corresponding Bézier control net.

The Bézier ordinates of this quadratic polynomial $\hat{p}_2$ are given by

$$b_{200} = d_3, \qquad b_{020} = d_7, \qquad b_{002} = d_{11}, \qquad b_{110} = c^e_{3,1}, \qquad b_{011} = c^e_{1,1}, \qquad b_{101} = c^e_{2,1}.$$

This results in

$$\begin{aligned} d_{31} &= z_1 d_3 + z_2 c^e_{3,1} + z_3 c^e_{2,1}, \qquad d_{33} = z_1 c^e_{3,1} + z_2 d_7 + z_3 c^e_{1,1}, \\ d_{35} &= z_1 c^e_{2,1} + z_2 c^e_{1,1} + z_3 d_{11}, \qquad d_{37} = z_1 d_{31} + z_2 d_{33} + z_3 d_{35}, \end{aligned} \tag{4.6}$$

and

$$\begin{aligned} d_{22} &= \lambda_{12} d_3 + \lambda_{21} c^e_{3,1}, \qquad d_{24} = \lambda_{12} c^e_{3,1} + \lambda_{21} d_7, \\ d_{23} &= \lambda_{12} d_{22} + \lambda_{21} d_{24}, \qquad d_{32} = \lambda_{12} d_{31} + \lambda_{21} d_{33}, \end{aligned} \tag{4.7}$$

and similar expressions for the remaining ordinates.

Only convex combinations are needed in the above computation of all Bézier ordinates of the PS3-spline in the form (3.1) starting from its spline coefficients. Evaluation or differentiation of the PS3-spline within each of the six subtriangles can then further be performed using the de Casteljau algorithm (see, e.g., Farin, 1986; Lai and Schumaker, 2007). This gives us a stable procedure to manipulate PS3-splines in its normalized B-spline representation.

More generally, if we apply the convex combinations (4.3), (4.5), (4.6) and (4.7) to the control points defined in (4.1), then we get directly the Bézier control points of the PS3-spline surface.

Fig. 7(left) shows a PS3-spline surface obtained as a discrete least-squares fit to the function $f(x, y) = \left(\exp\left((x-0.52)^2 + (y-0.48)^2\right) - 0.95\right)^{-1}$ on the domain $\Omega = [-1, 1] \times [-1, 1]$. The spline has been defined on the triangulation given in Fig. 5, and its Bézier control net is depicted in Fig. 7(right).

5. Some reduced spline spaces

In this section we provide some strategies to reduce the number of degrees of freedom in the PS3-spline space, i.e., $3n_v + 2n_e$. First, we describe the relation with the reduced Clough–Tocher (RCT3-) spline space considered by Speleers (2010b). Then, we provide a condensation strategy that maintains the full approximation order.

5.1. The relation with RCT3-splines

In Theorem 2 we have shown that the CT3-spline space is a subspace of the PS3-spline space. In particular, the RCT3-spline space considered by Speleers (2010b) is a subspace, so we can represent all its elements in terms of the PS3-spline basis. In this subsection we investigate how we can convert an RCT3-spline in its B-spline form into the PS3-spline form (3.1). We refer to Speleers (2010b) for more details on RCT3-splines and their properties.

Let s_{RCT} be an RCT3-spline in its B-spline form defined on the mesh Δ_{CT}, i.e.,

$$s_{RCT}(x, y) = \sum_{i=1}^{n_v} \sum_{j=1}^{3} c^{RCT}_{i,j} B^{RCT}_{i,j}(x, y). \tag{5.1}$$

For the conversion into the corresponding PS3-spline form, we assume that the partitions Δ_{CT} and Δ_{PS} are compatible, so that $\mathbb{S}^1_3(\Delta_{CT}) \subset \widehat{\mathbb{S}}^1_3(\Delta_{PS})$.

First, we set the PS3-triangles identical to the RCT3-triangles (see Speleers, 2010b, for details). From their construction it is clear that RCT3-triangles are always valid PS3-triangles. Indeed, focusing on the macro-triangle $\mathcal{T}(V_1, V_2, V_3)$ in Δ, the RCT3-triangle related to the vertex V_1 contains the points V_1, $(2V_1 + V_2)/3$ and $(2V_1 + V_3)/3$. Since both spline representations satisfy the same relations like (3.18) and (4.2), it follows that

$$c^v_{i,j} = c^{RCT}_{i,j}, \qquad i = 1, \ldots, n_v, \ j = 1, 2, 3. \tag{5.2}$$

Let us now concentrate on the edge $\varepsilon_k = \langle V_1, V_2\rangle$ of the macro-triangle $\mathcal{T}(V_1, V_2, V_3)$. The RCT3-spline s_{RCT} is a (single) cubic polynomial along this edge. Moreover, the directional derivative of s_{RCT} in a certain direction ν_k (not parallel to ε_k) is constrained to be a linear polynomial along the edge ε_k, i.e.,

$$\frac{\partial s_{RCT}}{\partial \nu_k}(R_k) = \lambda_{12}\frac{\partial s_{RCT}}{\partial \nu_k}(V_1) + \lambda_{21}\frac{\partial s_{RCT}}{\partial \nu_k}(V_2). \tag{5.3}$$

These two constraints will determine the values of the coefficients $c^e_{k,j}$, $j = 1, 2$.

A PS3-spline is a (single) cubic polynomial along the edge ε_k when we impose an additional C^3 super-smoothness across the edge $\langle Z, R_k\rangle$ with Z the split point of the macro-triangle $\mathcal{T}$. This is achieved when the parameter β, used in the construction of the Bernstein–Bézier representation of the PS3-spline (see (4.5)), satisfies

$$\beta = \frac{\lambda_{12}}{\lambda_{21}}(d_2 - \lambda_{12}d_1) + \frac{\lambda_{21}}{\lambda_{12}}(d_8 - \lambda_{21}d_5),$$

or, equivalently,

$$\beta = \lambda_{12}\left(s_{RCT}(V_1) + \frac{\|V_2 - V_1\|}{3}\frac{\partial s_{RCT}}{\partial \varepsilon_k}(V_1)\right) + \lambda_{21}\left(s_{RCT}(V_2) - \frac{\|V_2 - V_1\|}{3}\frac{\partial s_{RCT}}{\partial \varepsilon_k}(V_2)\right). \tag{5.4}$$

We now address the constraint (5.3). For the sake of simplicity of the presentation, we will focus on a particular case of interest (see Speleers, 2010b, Example 2.2), where

$$\nu_k = \frac{R_k - Z}{\|R_k - Z\|}.$$

It has been explained by Speleers (2010b) that this choice is favorable because the B-spline construction involves a less restrictive geometric constraint on the CT-refined triangulation. With this choice, we have

$$\frac{\partial s_{RCT}}{\partial \nu_k}(R_k) = \frac{3(d_{14} - d_{23})}{\|R_k - Z\|}, \qquad \frac{\partial s_{RCT}}{\partial \nu_k}(V_1) = \frac{3(d_2 - d_3)}{\|R_k - Z\|}, \qquad \frac{\partial s_{RCT}}{\partial \nu_k}(V_2) = \frac{3(d_8 - d_7)}{\|R_k - Z\|},$$

using the same notation for the Bézier ordinates as in Section 4.2. The constraint (5.3) implies

$$d_{14} - d_{23} = \lambda_{12}(d_2 - d_3) + \lambda_{21}(d_8 - d_7).$$

On the other hand, by the smoothness of the PS3-spline and by the relations (4.5)–(4.7), we get

$$\begin{aligned} d_{14} - d_{23} &= \lambda_{12}(d_{13} - d_{22}) + \lambda_{21}(d_{15} - d_{24}) \\ &= \lambda_{12}(\lambda_{12}(d_2 - d_3) + \lambda_{21}(\beta - c^e_{k,1})) + \lambda_{21}(\lambda_{12}(\beta - c^e_{k,1}) + \lambda_{21}(d_8 - d_7)) \\ &= {\lambda_{12}}^2(d_2 - d_3) + 2\lambda_{12}\lambda_{21}(\beta - c^e_{k,1}) + {\lambda_{21}}^2(d_8 - d_7). \end{aligned}$$

Taking into account that $\lambda_{21} = 1 - \lambda_{12}$, we obtain

$$\beta - c^e_{k,1} = \frac{1}{2}((d_2 - d_3) + (d_8 - d_7)) = \frac{\|R_k - Z\|}{6}\left(\frac{\partial s_{RCT}}{\partial \nu_k}(V_1) + \frac{\partial s_{RCT}}{\partial \nu_k}(V_2)\right).$$

Hence,

$$c^e_{k,1} = \beta - \frac{\|R_k - Z\|}{3}\beta^\nu, \qquad \text{with} \qquad \beta^\nu = \frac{1}{2}\left(\frac{\partial s_{RCT}}{\partial \nu_k}(V_1) + \frac{\partial s_{RCT}}{\partial \nu_k}(V_2)\right). \tag{5.5}$$

From the definition of β in (4.4) we can compute the value of $c^e_{k,2}$, which depends on the type of the edge ε_k.

1. If ε_k is a boundary edge, then

$$c^e_{k,2} = \beta. \tag{5.6a}$$

2. If ε_k is an interior edge, then

$$c^e_{k,2} = \frac{\|Z - \widetilde{Z}\|}{\|Z - R_k\|}\beta - \frac{\|R_k - \widetilde{Z}\|}{\|Z - R_k\|}c^e_{k,1} = \beta + \frac{\|R_k - \widetilde{Z}\|}{3}\beta^v. \tag{5.6b}$$

The coefficients in (5.2) and (5.5)–(5.6) with β given in (5.4) constitute the PS3-spline representation (3.1) of the RCT3-spline s_{RCT} in (5.1).

5.2. Full approximation with less degrees of freedom

In the previous subsection we have detailed a strategy to reduce the number of degrees of freedom to $3n_v$. Indeed, by choosing the edge coefficients $c^e_{k,j}$ as in (5.5)–(5.6) with β given in (5.4), we only keep the vertex coefficients $c^v_{i,j}$ as degrees of freedom. Unfortunately, it is known that this choice has a negative impact on the approximation order (the order is decreased by one).

We now discuss how we can reduce the number of degrees of freedom, while maintaining the full approximation order. Instead of the RCT3-spline space, we could consider the (complete) CT3-spline space. We have seen in Theorem 2 that the CT3-spline space is also a subspace of the PS3-spline space. This subspace has optimal approximation order, while its dimension is smaller, namely $3n_v + n_e$. A CT3-spline is obtained by imposing an additional C^3 super-smoothness along each edge in Δ. From Section 5.1 we know that this is achieved by requiring the condition (5.4) for each edge e_k, $k = 1, \ldots, n_e$.

Alternatively, inspired by Kashyap (1996) and Mann (1999), the edge coefficients could be determined from the vertex coefficients by means of the following local two-step strategy, in case e_k is an interior edge of Δ.

1. Use the Hermite data at the vertices (provided by the vertex coefficients $c^v_{i,j}$, see (4.2)) of the two triangles sharing the edge e_k to compute a cubic polynomial by least-squares fitting (or any other approximation method with cubic precision).
2. Compute the coefficients $c^e_{k,j}$ related to the edge e_k based on this cubic polynomial such that the resulting spline has cubic precision.

The second step can be implemented as follows. Let us denote by q the cubic polynomial obtained after fitting the Hermite data at the vertices V_1, V_2, V_3, V_4. Then, suppose that the Bernstein–Bézier form of q over the triangle $\mathcal{T}(V_1, V_2, V_3)$ is given by the Bézier ordinates b_{ijk}, $i + j + k = 3$. Moreover, suppose that the Bernstein–Bézier form of q over the adjacent triangle $\widetilde{\mathcal{T}}(V_1, V_2, V_4)$ is given by the Bézier ordinates $\tilde{b}_{ijk}$, $i + j + k = 3$. Then, we may choose

$$\begin{aligned} c^e_{k,1} &= z_1 b_{210} + z_2 b_{120} + z_3 b_{111}, \\ c^e_{k,2} &= \tilde{z}_1 \tilde{b}_{210} + \tilde{z}_2 \tilde{b}_{120} + \tilde{z}_3 \tilde{b}_{111}, \end{aligned}$$

where (z_1, z_2, z_3) are the barycentric coordinates of the split point Z with respect to $\mathcal{T}$, and $(\tilde{z}_1, \tilde{z}_2, \tilde{z}_3)$ are the barycentric coordinates of the split point $\widetilde{Z}$ with respect to $\widetilde{\mathcal{T}}$. One can verify that this choice will reproduce cubic polynomials, and so maintain the optimal approximation order.

6. Concluding remarks

In this paper we have presented a new C^1 cubic spline space defined over a triangulation endowed with a PS-refinement. Thanks to the locally imposed C^2 super-smoothness, the proposed PS3-spline space has a simple dimension formula, namely $3n_v + 2n_e$, and the space is a close extension of the classical CT3-spline space. In addition, we have constructed a normalized B-spline basis for this space. The basis functions have a local support, they are nonnegative, and they form a partition of unity. We have also described how to compute from the control points of a PS3-spline its corresponding Bézier control net in a stable way.

In the literature one finds few other normalized B-spline representations for C^1 cubic splines on triangulations with a macro-structure. For example, such a representation exists for RCT3-splines (Speleers, 2010b) and for cubic PS-splines with a different super-smoothness (Lamnii et al., 2014). For the sake of convenience, the latter splines will be referred to as PS3$^{\maltese}$-splines in the following. The proposed new cubic B-spline representation has some favorable properties with respect to the other ones.

- The full space of cubic polynomials belongs to the PS3-spline space. This is also the case for the PS3$^{\maltese}$-spline space, whereas the RCT3-spline space only contains the full space of quadratic polynomials. This implies that PS3-splines and PS3$^{\maltese}$-splines possess full approximation power but RCT3-splines do not.
- CT3-splines (and RCT3-splines) are in the PS3-spline space (on condition that the partitions are compatible, see Theorem 2), so they can be represented in the PS3-spline form (3.1). This is not the case for the PS3$^{\maltese}$-spline space.

- The PS3 Hermite interpolation problem (see Theorem 1) only involves first derivatives, and not second derivatives like in the PS3$^{\maltese}$-spline case. The use of higher order derivatives is not so appealing in approximation. In addition, it might simplify the construction of quasi-interpolation schemes (see, e.g., Lamnii et al., 2014; Sbibih et al., 2014; Speleers, 2015).
- The construction of the PS3-spline basis involves the use of PS3-triangles. These triangles are required to contain a specific set of PS3-points (see Theorem 3). Because this constraint is less restrictive, the PS3-triangles can be chosen smaller than the corresponding triangles for RCT3-splines and PS3$^{\maltese}$-splines. This implies that the PS3 control points will be closer to the PS3-spline surface.

We now make a comparison with the spaces $\mathbb{S}_3^1(\Delta_{CT})$ and $\mathbb{S}_3^1(\Delta_{PS})$, defined in (2.5) and (2.6), respectively, and we give an outlook on the construction of a normalized B-spline basis for them.

- The space $\mathbb{S}_3^1(\Delta_{PS})$ is an extension of the PS3-spline space, so it shares the full approximation power but it has a larger dimension, namely $3n_v + 4n_e$. A normalized B-spline basis can be constructed for this space by adopting the techniques from Dierckx (1997) and Speleers (2010a, 2013a).
- The space $\mathbb{S}_3^1(\Delta_{CT})$ is contained in the PS3-spline space (see one of the previous items). It is known that it has full approximation power, but it is not clear whether a normalized B-spline basis can be constructed or not for this space in general. Since its dimension is $3n_v + n_e$, it is natural to associate three basis functions with each vertex and one basis function with each edge. For the construction of the vertex basis functions, one could follow the approach from Speleers (2010b) for RCT3-splines. It seems impossible, however, to construct a nonnegative basis function related to an interior edge with support on two macro-triangles (the triangles adjacent to the edge). This would imply that possible edge basis functions must have larger support.

Finally, in Section 5, we have provided some strategies to reduce the number of degrees of freedom in the PS3-spline space. In particular, we have shown that we can easily convert an RCT3-spline in its B-spline form (5.1) into the PS3-spline form (3.1). Note that only the condition (5.4) is required to obtain a general CT3-spline in the PS3-spline form.

Acknowledgements

This work was supported by the MIUR 'Futuro in Ricerca 2013' Programme through the project DREAMS and by the 'Uncovering Excellence' Programme of the University of Rome 'Tor Vergata' through the project DEXTEROUS.

References

Alfeld, P., Schumaker, L.L., 2002a. Smooth macro-elements based on Clough–Tocher triangle splits. Numer. Math. 90, 597–616.
Alfeld, P., Schumaker, L.L., 2002b. Smooth macro-elements based on Powell–Sabin triangle splits. Adv. Comput. Math. 16, 29–46.
Chen, S.K., Liu, H.W., 2008. A bivariate C^1 cubic super spline space on Powell–Sabin triangulation. Comput. Math. Appl. 56, 1395–1401.
Clough, R.W., Tocher, J.L., 1965. Finite element stiffness matrices for analysis of plates in bending. In: Conf. on Matrix Methods in Structural Mechanics. Wright Patterson Air Force Base, Ohio, pp. 515–545.
Dierckx, P., 1997. On calculating normalized Powell–Sabin B-splines. Comput. Aided Geom. Des. 15, 61–78.
Dierckx, P., Van Leemput, S., Vermeire, T., 1992. Algorithms for surface fitting using Powell–Sabin splines. IMA J. Numer. Anal. 12, 271–299.
Farin, G., 1985. A modified Clough–Tocher interpolant. Comput. Aided Geom. Des. 2, 19–27.
Farin, G., 1986. Triangular Bernstein–Bézier patches. Comput. Aided Geom. Des. 3, 83–127.
Kashyap, P., 1996. Improving Clough–Tocher interpolants. Comput. Aided Geom. Des. 13, 629–651.
Laghchim-Lahlou, M., Sablonnière, P., 1994. Triangular finite elements of HCT type and class C^ρ. Adv. Comput. Math. 2, 101–122.
Lai, M.J., Schumaker, L.L., 2001. Macro-elements and stable local bases for splines on Clough–Tocher triangulations. Numer. Math. 88, 105–119.
Lai, M.J., Schumaker, L.L., 2003. Macro-elements and stable local bases for splines on Powell–Sabin triangulations. Math. Comput. 72, 335–354.
Lai, M.J., Schumaker, L.L., 2007. Spline Functions on Triangulations. Cambridge University Press.
Lamnii, M., Mraoui, H., Tijini, A., Zidna, A., 2014. A normalized basis for C^1 cubic super spline space on Powell–Sabin triangulation. Math. Comput. Simul. 99, 108–124.
Maes, J., Bultheel, A., 2006. Stable multiresolution analysis on triangles for surface compression. Electron. Trans. Numer. Anal. 25, 224–258.
Mann, S., 1999. Cubic precision Clough–Tocher interpolation. Comput. Aided Geom. Des. 16, 85–88.
Manni, C., Sablonnière, P., 2007. Quadratic spline quasi-interpolants on Powell–Sabin partitions. Adv. Comput. Math. 26, 283–304.
Nürnberger, G., Zeilfelder, F., 2000. Developments in bivariate spline interpolation. J. Comput. Appl. Math. 121, 125–152.
Powell, M.J.D., Sabin, M.A., 1977. Piecewise quadratic approximations on triangles. ACM Trans. Math. Softw. 3, 316–325.
Sablonnière, P., 1985. Composite finite elements of class C^k. J. Comput. Appl. Math. 12&13, 541–550.
Sbibih, D., Serghini, A., Tijini, A., 2009. Polar forms and quadratic spline quasi-interpolants on Powell–Sabin partitions. Appl. Numer. Math. 59, 938–958.
Sbibih, D., Serghini, A., Tijini, A., 2012. Normalized trivariate B-splines on Worsey–Piper split and quasi-interpolants. BIT Numer. Math. 52, 221–249.
Sbibih, D., Serghini, A., Tijini, A., 2015. Superconvergent quadratic spline quasi-interpolants on Powell–Sabin partitions. Appl. Numer. Math. 87, 74–86.
Sbibih, D., Serghini, A., Tijini, A., Zidna, A., 2014. Superconvergent C^1 cubic spline quasi-interpolants on Powell–Sabin partitions. BIT Numer. Math. http://dx.doi.org/10.1007/s10543-014-0523-z. In press.
Speleers, H., 2010a. A normalized basis for quintic Powell–Sabin splines. Comput. Aided Geom. Des. 27, 438–457.
Speleers, H., 2010b. A normalized basis for reduced Clough–Tocher splines. Comput. Aided Geom. Des. 27, 700–712.
Speleers, H., 2013a. Construction of normalized B-splines for a family of smooth spline spaces over Powell–Sabin triangulations. Constr. Approx. 37, 41–72.
Speleers, H., 2013b. Multivariate normalized Powell–Sabin B-splines and quasi-interpolants. Comput. Aided Geom. Des. 30, 2–19.
Speleers, H., 2015. A family of smooth quasi-interpolants defined over Powell–Sabin triangulations. Constr. Approx. 41, 297–324.

Speleers, H., Dierckx, P., Vandewalle, S., 2006. Numerical solution of partial differential equations with Powell–Sabin splines. J. Comput. Appl. Math. 189, 643–659.

Speleers, H., Dierckx, P., Vandewalle, S., 2009. Quasi-hierarchical Powell–Sabin B-splines. Comput. Aided Geom. Des. 26, 174–191.

Speleers, H., Manni, C., Pelosi, F., Sampoli, M.L., 2012. Isogeometric analysis with Powell–Sabin splines for advection–diffusion–reaction problems. Comput. Methods Appl. Mech. Eng. 221–222, 132–148.